Energy-Efficient Train Timetabling

Goverde, Rob M.P.; Scheepmaker, Gerben M.

DOI
10.1007/978-3-031-34656-9_4

Publication date
2023

Document Version
Final published version

Published in
Energy-Efficient Train Operation

Chapter 4
Energy-Efficient Train Timetabling

Rob M. P. Goverde and Gerben M. Scheepmaker

4.1 Introduction

The aim of energy-efficient train timetabling is to construct a timetable that enables energy-efficient train operation. The train timetabling problem determines for each train the arrival and departure times at all stations or other timing points, while considering track capacity constraints such that the resulting train paths are conflict-free [7, 21]. The energy consumption of the trains depends on the allocation of the time allowances over the timetable. First, the distribution of running time supplement over a train path affects the train driving behaviour and therefore the energy consumption. Second, the allocation of buffer times between the scheduled train paths determines the robustness of a timetable, such that small delays do not immediately result in path conflicts. This avoids an increase in energy consumption due to braking or unplanned stops followed by re-acceleration and running faster to recover the time loss.

In the train timetabling problem the train paths for all train services are scheduled and coordinated aiming at a conflict-free allocation of trains to the railway capacity. A train path is the time-distance allocation of a train service to a specific sequence of tracks and station platforms over the railway infrastructure, including the arrival and departure times at the stations, as well as possible additional passage times at intermediate timing points. The majority of the literature on train timetabling is about computing feasible and robust timetables for given lower and upper bounds on the activity times, such as dwell times at stations, running times between stations, transfer times between connecting trains at stations, and minimum headway times between event times of adjacent train paths [7, 21]. The running times are usually

R. M. P. Goverde (✉)
Department of Transport and Planning, Delft University of Technology, Delft, Netherlands
e-mail: R.M.P.Goverde@tudelft.nl

G. M. Scheepmaker
Netherlands Railways, Utrecht, Netherlands
e-mail: gerben.scheepmaker@ns.nl

S. Su et al., *Energy-Efficient Train Operation*, Lecture Notes in Mobility,
https://doi.org/10.1007/978-3-031-34656-9_4

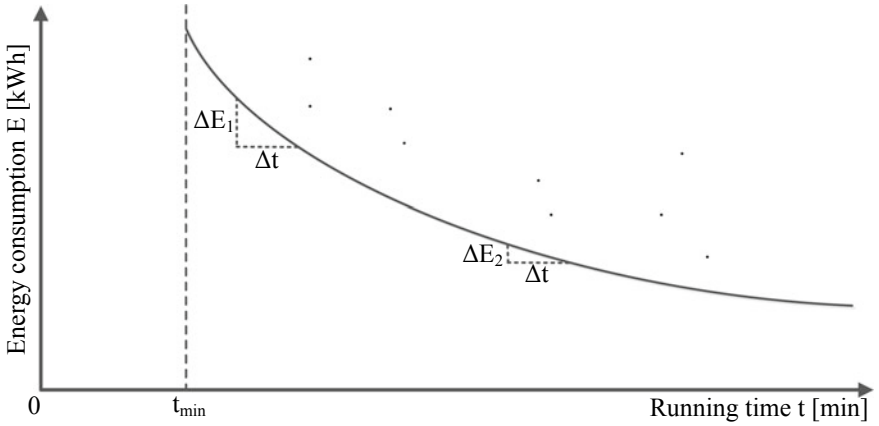

Fig. 4.1 Pareto front of energy consumption versus running time

fixed or given some flexibility, based on an external running time calculation for the minimum technical running time and norms for the running time supplement. Optimization of the nominal timetable usually aims at minimizing the travel times (including dwell and transfer times), while the robust train timetabling problem aims at reducing delay propagation by including sufficient buffer times between the train paths. The optimization of both the nominal and robust train timetabling problem thus focuses on the time domain, while the impact of changes in running times to the speed profiles and therefore to energy consumption, either negative or positive, is mostly discarded. Likewise, the impact of a change in running time to the minimum headway times is also hardly considered in the existing literature, which would also require a microscopic level of detail similar to train trajectory optimization.

The amount of scheduled running time determines the running time supplement available for energy-efficient driving. The minimum running time corresponds to running as fast as possible considering the train and track characteristics and respecting all operational constraints, which also leads to the highest energy consumption. Running time supplement is added to increase the stability of the timetable by (1) reducing the occurrence of primary delays due to train parameter variations and external (weather) conditions by which a train needs more time than scheduled, and (2) recovering existing delays by running faster than scheduled [13]. The added running time supplement must be translated into a 'slower' speed profile that covers the scheduled running time and cumulatively determines the running time over the entire train path. The exact speed profile determines the resulting energy consumption.

Figure 4.1 shows a typical Pareto front corresponding to the trade-off between energy consumption and running time. The energy consumption is the highest for the minimum running time $t_{\min}$. For larger running times the energy consumption depends on the driving behaviour. The Pareto front corresponds to the energy-efficient speed profiles, which dominate other solutions associated to non-optimal driving (indicated by the dots). The decreasing Pareto curve illustrates that increasing the

running time leads to energy savings, but this effect decreases for larger running times, i.e., increasing the running time by some amount Δt will lead to a larger energy saving ΔE_1 than the energy saving ΔE_2 obtained by a further increase by the same amount when already supplement is included, $\Delta E_1 > \Delta E_2$. These Pareto curves can be used to find the optimal allocation of running time supplements over multiple stops, by first generating the Pareto fronts for all train runs between two stops (or other timing points) and then selecting the running times from the Pareto curves to the train runs such that the total energy is minimized [3, 9, 11, 31–33, 38]. The first step can be done by solving the energy-efficient train trajectory optimization problem between two stops for various running times for each train path segment, while the second step can be done using dynamic programming [3] or direct search algorithms.

A train trajectory optimization model can also be used to compute the optimal energy-efficient speed profile over multiple stops directly, including the optimal arrival and departure times at the intermediate stops [6, 30, 35, 36]. When multiple trains are considered track capacity constraints must be modelled, which can take the form of default headway times at arrivals and departures as in macroscopic train timetabling problems [19, 35, 36, 41] or dynamic minimum headway times computed after the train trajectories have been computed [28, 40]. An alternative optimization model integrates the train timetabling and speed profile problem in a space-time-speed network, where the speed profiles are linearized or otherwise simplified to keep the resulting optimization problem tractable [40, 43]. As dwell (and transfer) times are a main source of disturbances or delays affecting the remaining running time supplement for energy-efficient driving, also models have been proposed to include stochastic or fuzzy dwell times in the train trajectory optimization problem over multiple stops [6, 9, 15], while other models include passenger flows over the network [19, 39, 41]. For an extensive literature review of energy-efficient train timetabling, see Scheepmaker et al. [29].

In general, energy-efficient train timetabling leads to multi-objective optimization problems. Goverde et al. [15] developed a sequential approach for the multiple-objective timetable optimization problem on a network, where the first aim is to determine a conflict-free, stable and robust timetable. A micro-macro iterative model was developed to compute an optimal network timetable, where the macroscopic level optimizes a trade-off between travel times and robustness, and the microscopic level guarantees feasibility and stability using blocking time theory [22]. In a third step, energy-efficient speed profiles are embedded over the corridors between main stations, maintaining the scheduled departure and arrival times at the corridor ends and including stochastic dwell time distributions at intermediate stops. Scheepmaker and Goverde [28] proposed a multi-objective optimization problem for computing an energy-efficient train timetable on a heterogeneous traffic corridor considering the joint objectives of total running time, infrastructure occupation, robustness, and energy consumption. They first computed the energy-efficient train trajectories for a range of scheduled running times for each train type, followed by computing the associated microscopic blocking times. The latter were used to compute the minimum line headway times to guarantee conflict-free train paths and the infrastructure

occupation to guarantee sufficient buffer time for robustness. The problem was then solved using the weighted-sum method.

Modern electric trains can apply regenerative braking using the engine as generator to convert kinetic energy into electricity. This regenerated energy can be used within the train (for lighting, heating, ventilation and air conditioning), stored in batteries, or fed back to the power supply system to be used by nearby trains [12]. In general, however, power is lost due to generated heat and the efficiencies of the engine, converters, energy storage device and/or the power supply system, depending on specific conditions. In this chapter, we exclude energy gains by regenerative braking, while similar results are obtained when regenerative braking is included in the objective function, see Scheepmaker and Goverde [27]. The main uncertainty is the determination of the regenerative braking efficiency, which requires detailed modelling of the energy storage system (see Chap. 6) or simulation of the power supply network (see Chap. 7). When regenerative braking is used, synchronization of arrival and departure times can increase the efficiency of reused regenerative braking energy by nearby accelerating trains, which will be considered in Chap. 5. In the present chapter, we focus on facilitating energy-efficient driving of each train separately without dynamic coordination or cooperation with other trains.

This chapter focuses on the modelling of train trajectory optimization problems for energy-efficient train timetabling. Algorithms for solving the optimal control problems based on the application of Pontryagin's Maximum Principle [1, 2, 16] are presented in Chap. 3. The examples in this chapter were all solved by a pseudospectral method using Pontryagin's Maximum Principle for validation [16, 34].

The structure of this chapter is as follows. Section 4.2 first considers the minimum-time train trajectory problem which is used as a reference driving strategy and applied in practice when a train is delayed. Section 4.3 considers the energy-efficient train trajectory optimization problem between two stops. This is extended in Sect. 4.4 to energy-efficient train trajectory optimization over multiple stops, where the running times between successive stops are optimized. Section 4.5 then continues with energy-efficient train timetabling over corridors with multiple trains. Finally, conclusions on energy-efficient train timetabling are presented in Sect. 4.6.

4.2 Minimum Running Time Calculation

4.2.1 Problem Formulation

The minimum running time is the technical running time that a train needs to traverse a given route between two timing points as fast as possible, while considering the basic characteristics of the train and track. It assumes default values for the train and track parameters representing good conditions, such as good weather conditions and constant power supply. The minimum running time is the basis for determining the scheduled running times in the timetable and it is assumed to be achievable when a

train is running late. Therefore, the minimum running time is essential information for both timetable planning and operational traffic management. This section will focus on the minimum running time between two station stops. Minimum running times between arbitrary timing points, such as signals, junctions or non-served stations, are obtained in a similar way with a positive speed specified instead of standstill at a station platform track.

The minimum running time calculation is based on data about the train, track and operations:

- Train characteristics: mass, length, maximum speed, resistance, traction, brake,
- Route-specific track characteristics: speed limits, gradients, curves, tunnels,
- Operational characteristics: planned stops, signalling.

A train consists of a formation of one or more coupled rolling stock units, which may be either self-propelled multiple units or locomotives with carriages. The train characteristics therefore depend on a specific train composition, such as train length and mass. The traction, or tractive effort, $F(v)$ [N] is the sum of all tractive forces at the driving wheels and is speed-dependent. It is usually given as a nonlinear tractive effort curve in a force-speed diagram that represents the maximum tractive effort $F^{\max}(v)$ as a function of speed v [m/s]. The curve typically includes a constant part at low speeds corresponding to the adhesion limit, and a hyperbolic part corresponding to the maximum power P [W] at higher speeds due to the relationship $F^{\max} = P/v$ until the maximum speed $v^{\max}$. The train resistance R [N] consists of rolling and air resistance which together form a a second-order polynomial of speed $R(v) = a + bv + cv^2$, with with non-negative coefficients $a, b \geq 0$ and $c > 0$, known as the Davis equation [10]. The mechanical braking characteristics are often given by a constant braking rate or a step function of braking rates as function of speed $B(v)$ [N] that models the maximum (service) braking. Also detailed formulae exist with parameters including a braking percentage and brake build-up time. In addition to mechanical braking, regenerative braking can be considered using the engine as generator, which can be modelled as a nonlinear function of speed like the opposite of the maximum tractive effort curve. Without loss of generality, we exclude regenerative braking in this chapter, but similar results are obtained when regenerative braking is included in the objective function [27]. Certain assumptions have to be made for the computation of the minimum running time, such as train mass for a typical passenger load, train resistance parameters for good weather conditions, and tractive forces for a given constant power supply.

An accurate running time calculation requires input about the planned route with the associated track description including the static speed profile, gradient profile, curve profile, tunnel sections, and possible other special sections such as power supply changes in electric railways. The gradients, curves and tunnels add additional line resistances to the train movement. The gradient profile is usually assumed to be a step function of distance corresponding to successive track sections with constant gradient. The gradient resistance for a slope with angle α is $G(s) = gm \sin\alpha \approx gmn$ [N], with $g = 9.81$ m/s^2 the acceleration due to gravity, m the train mass, and n [m/km] the change in vertical height with horizontal distance.

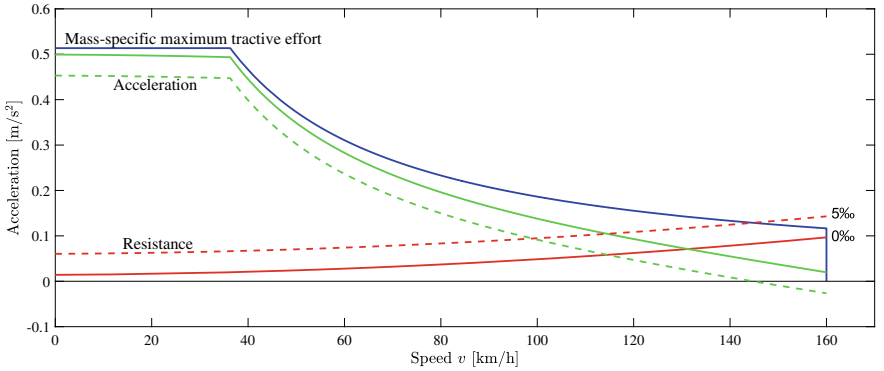

Fig. 4.2 Acceleration-speed diagram of mass-specific maximum tractive effort (blue), resistance and resulting acceleration for flat track (solid red and green) and $5^0/_{00}$ gradient (dashed red and green)

The force available for acceleration, known as the surplus force or acceleration force, is given by the force equilibrium of tractive effort minus total resistance (including line resistance of slopes, curves and tunnels) and includes a dimensionless rotating mass factor ρ,

$$\rho ma = F(s) - R(v) - G(s).$$

Instead of forces, it is convenient to consider the mass-specific forces that are obtained by dividing the forces by a factor ρm, which results in acceleration units m/s^2, and

$$a = (F(v) - R(v) - G(s))/(\rho m) = f(v) - r(v) - g(s).$$

Figure 4.2 shows an acceleration-speed diagram illustrating typical curves for mass-specific maximum tractive effort $f^{\max}(v)$ and resistance $r(v) - g(s)$, and the resulting mass-specific surplus force or acceleration $a(v)$. It clearly shows that acceleration is a nonlinear function of speed that decreases towards zero for larger speeds. The maximum braking rate for this train type is -0.66 m/s^2, illustrating that train acceleration is even much slower than braking. The acceleration curve on an incline with $5^0/_{00}$ shows that the maximum speed can even be limited on uphill slopes, although the maximum speed of this train type is limited to 140 km/h.

The static speed profile is a step function of distance that includes line speed limits and possible route-dependent speed restrictions due to reverse switches leading to a different track. Locations on the route affecting the operational speed must also be specified, such as the stop position of the train front at platform tracks (that may depend on the train length or number of carriages), and possible trackside signs or signals with a brake indication such as at the entry of stations. Moreover, the actual train behaviour depends on operational rules, such as starting with full acceleration only after the entire train has passed a reverse switch section and braking according to the requirements of the automatic train protection. For instance, with modern

distance-to-go braking curve supervision, such as in the European Train Control System (ETCS), braking can start at the last moment before a location with a restricted (or zero) speed as long as the permitted braking curve is not exceeded. In contrast, in a traditional three-aspect fixed-block signalling system a train may need to start braking when passing a yellow approach signal and proceed with a restricted speed until a final braking regime to reach standstill at the stop position.

The minimum running time calculation can now be formulated as an optimal control problem. The minimum time train control (MTTC) problem from initial position s_0 to final position s_1 is then formulated as follows:

$$\text{Minimize } t(s_1) \tag{4.1}$$

subject to the constraints

$$\dot{t}(s) = 1/v(s) \tag{4.2}$$
$$\dot{v}(s) = (u(s) - r(v) - g(s))/v(s) \tag{4.3}$$
$$0 \le v(s) \le v^{\max}(s) \tag{4.4}$$
$$u^{\min}(v) \le u(s) \le u^{\max}(v) \tag{4.5}$$
$$t(s_0) = 0,\ v(s_0) = 0,\ v(s_1) = 0, \tag{4.6}$$

while the final time $t(s_1)$ is free. The independent variable is distance s [m], the state variables are time t [s] and speed v [m/s], $\dot{t} = dt/ds$ and $\dot{v} = dv/ds$ denote the derivatives of the state variables with respect to the independent variable s, and the control variable u [m/s^2] is the mass-specific applied (tractive or braking) force $u(s) = F(s)/(\rho m)$, i.e., the applied force divided by total mass including a rotating-mass factor ρ. The control is bounded between a maximum braking rate $u^{\min} = B/(\rho m) < 0$ and a maximum specific traction force $u^{\max} = F^{\max}/(\rho m) = \min(u_0, p^{\max}/v)) \ge 0$, with mass-specific adhesion limit u_0 and mass-specific maximum traction power $p^{\max} = P/(\rho m)$ [m^2/s^3] using the relation $p^{\max} = u^{\max} v$. Note that traction and braking cannot be used at the same time. We use the notation $u^+(s) = \max(u(s), 0) \ge 0$ and $u^-(s) = \min(u(s), 0) \le 0$ so that $u(s) = u^+(s) + u^-(s)$. The resistance forces consist of a mass-specific train resistance $r(v) = R(v)/(\rho m)$ [m/s^2] and a mass-specific line resistance $g(s) = G(s)/(\rho m)$ [m/s^2]. Finally, the speed is bounded above by a speed limit $v^{\max}(s)$, which is assumed piecewise constant.

An alternative model could be provided with time as independent variable, and distance and speed as time-dependent state variables, which would lead to more conventional differential equations to time. However, it is more convenient to use distance as independent variable according to the track-oriented constraints such as the static speed and gradient profiles that are stepwise functions of distance.

4.2.2 Optimality Conditions

According to Pontryagin's Maximum Principle [24], the optimal control should maximize the Hamiltonian H defined as

$$H(t, v, \lambda_1, \lambda_2, u, s) = \lambda_1/v + \lambda_2 \left(u - r(v) - g(s)\right)/v, \tag{4.7}$$

where λ_1 and λ_2 are the co-state variables corresponding to time and speed, respectively. In the case of free final time, $\lambda_1 \equiv -1$, and λ_2 is a nonlinear function of the independent variable s [16]. This Hamiltonian is linear in the control u with coefficient λ_2/v. The optimal control structure $\hat{u}$ is therefore obtained from the sign of λ_2 as (1) maximum traction $u^{\max}(v(s))$ if $\lambda_2(s) > 0$, (2) cruising at the maximum speed using partial traction $r(v^{\max}(s)) + g(s)$ if $\lambda_2(s) = 0$, and (3) maximum braking $u^{\min}(v(s))$ if $\lambda_2(s) < 0$. This leads to the following optimal control structure [16]:

$$\hat{u}(s) = \begin{cases} u^{\max}(v(s)) & \text{if } \lambda_2(s) > 0 \text{ (Maximum acceleration)} \\ r(v^{\max}(s)) + g(s) & \text{if } \lambda_2(s) = 0 \text{ (Cruising at maximum speed)} \\ u^{\min}(v(s)) & \text{if } \lambda_2(s) < 0 \text{ (Maximum braking).} \end{cases} \tag{4.8}$$

The switching points between the three driving regimes are determined by the dynamics of the co-state variable λ_2 that satisfies an adjoint differential equation [16]. However, from the optimal control structure (4.8) a constructive method can be derived without the need to calculate the co-state λ_2 explicitly, which defines the fastest running: accelerate as fast as possible until the maximum speed is obtained, maintain the maximum speed as long as possible, and brake as fast as possible at the end to a standstill at the final destination s_1. Cruising at the maximum speed generally implies applying partial traction to counter the resistances at the maximum speed. On steep downhill slopes, where the speed increases even when not applying any traction, partial braking must be applied to maintain at the maximum speed. For safety reasons, the negative gradients should be limited such that maximum braking should prevent exceeding the maximum speed. If the static speed profile includes one or more intermediate speed restrictions then the train should brake as late as possible before the speed restriction and re-accelerate as early as possible again to a higher speed when possible. In case of steep uphill slopes where even full traction cannot keep the maximum cruising speed, the optimal control switches to maximum acceleration until the maximum speed is reached again (after the gradient has become less steep). In case of any restrictions from the signalling system the maximal permitted speed curves should be followed. Hence, this optimal control structure is completely aligned with the common technical running time calculation.

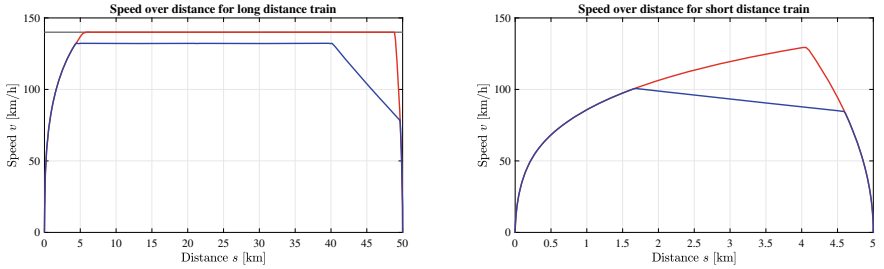

Fig. 4.3 Speed-distance diagrams for the minimum-time (red) and energy-efficient train control (blue) of a long-distance train (left) and a short-distance train (right)

4.2.3 Illustrative Example

Figure 4.3 shows speed-distance diagrams for typical minimum-time train trajectories for a long-distance train (left) and a short-distance train (right) on flat track. Also shown are the corresponding energy-efficient trajectories, which will be explained in the next section.

The minimum-time speed profile on the left shows a train accelerating to the speed limit $v^{\max} = 140$ km/h with maximal tractive effort bounded by the maximum traction-speed curve, then cruising at the speed limit using partial traction to counter the train and line resistances, and finally braking at the maximum braking rate to a standstill at the final position. This speed profile is similar for routes with non-steep gradients. Only the energy consumption would change due to varying partial traction in the cruising regime as opposed to a constant partial traction setting on flat track.

The speed-distance diagram on the right in Fig. 4.3 illustrates the minimum-time speed profile over a short stop distance. In this case, the distance is too short to reach the speed limit. The train now applies maximum acceleration until it hits the braking curve at which the control switches to maximum braking in order to reach standstill at the stop.

4.3 Energy-Efficient Train Trajectory Optimization Between Stops

4.3.1 Problem Formulation

In practice, scheduled running times consist of the minimum running time plus a running time supplement. The running time supplement serves various purposes:

1. To cover variations in the train parameters that will lead to larger running times,
2. To cover less favorable conditions such as strong headwind,
3. To compensate for variations in driver behavior,

4. To round up to full minutes (or any other time unit),
5. To fit the train path in the timetable at bottlenecks,
6. To reduce traction energy consumption,
7. To enable delay recovery.

The first three points relate to reliability of the scheduled running time. If the minimum running time would be used in timetables then delays will occur often as individual rolling stock will have (slightly) varying characteristics due to different states of wear. Furthermore, operational conditions may vary with fluctuating passenger flows and weather conditions, and also the driver behavior varies from day to day and between different drivers. Also the actual train composition may differ from the one used in the calculation of the minimum running time, which specifically holds for periodic timetables where the same scheduled running time is used for all trains from a specific train line throughout a day, while in practice the train length (and hence composition) is varied to accommodate fluctuating passenger demand over the day. In principle, the minimum running time could be computed for the worst-case train composition and conditions, but this will also lead to implicit running time supplements for those trains running with better train compositions and conditions. Therefore, the minimum running time is usually computed based on average parameter values and then a regular running time supplement is defined as a percentage of the computed minimum running time. Typical regular running time supplements are 5%–10% depending on specific rules from different railways or countries, which may differentiate for instance between short and long distance trains. In addition to this percentage, an additional absolute time supplement may be added for rounding or 'bending' the train path to fit between other train paths according to the 4th and 5th mentioned points.

Given a scheduled running time including running time supplement, the speed profile should be adapted for on-time running. This gives opportunities for energy-efficient driving which is thus considered as a secondary objective. In addition, if a train is running late then it could run faster to recover the delay by the actual running time supplement, which further improves punctuality and service stability. However, note that worst-case trains and conditions might actually need the full running time supplement, and thus do not have this recovery opportunity. Therefore, the actual combination of relative and absolute running time supplement is a design choice to enable reliable train services regarding both parameter variations and delay recovery. In particular, extra supplements may be planned just before bottlenecks or main stations to allow improved on-time running at these strategic locations. However, it then becomes very important that trains do not arrive early at these locations and disturb other trains, so that computing a feasible speed profile covering the entire scheduled running time under normal conditions remains essential.

The actual running time supplement may also be affected by a (slight) initial departure delay, which essentially reduces the actual available running time. Hence, optimal operational speed profiles may be computed depending on specific train characteristics and the available running time consisting of the scheduled running time minus any initial departure delay.

The energy-efficient train control problem or train trajectory optimization problem is the problem of finding the optimal train trajectory for a train run between two stops in a given scheduled time T [s] such that the total traction energy is minimized. The traction energy can be computed as the integral of the applied traction over distance. Hence, the objective function is

$$\text{Minimize} \int_{s_0}^{s_1} u^+(s)ds \tag{4.9}$$

under the constraints (4.2)–(4.5) and the boundary conditions

$$t(s_0) = 0, t(s_1) = T, v(s_0) = 0, v(s_1) = 0. \tag{4.10}$$

Note that in contrast to (4.6) the final time is given.

4.3.2 Optimality Conditions

According to Pontryagin's Maximum Principle [24] the optimal control should maximize the Hamiltonian H which is defined for this problem as

$$\begin{aligned} H(t, v, \lambda_1, \lambda_2, u, s) &= -u^+ + \lambda_1/v + \lambda_2(u - r(v) - g(s))/v \\ &= \begin{cases} (\lambda_2/v - 1)u + (\lambda_1 - \lambda_2 r(v) - \lambda_2 g(s))/v & \text{if } u \geq 0 \\ (\lambda_2/v)u + (\lambda_1 - \lambda_2 r(v) - \lambda_2 g(s))/v & \text{if } u < 0, \end{cases} \end{aligned} \tag{4.11}$$

with λ_1 and λ_2 the co-state variables associated to time and speed, respectively. The co-state variable λ_1 is a negative constant which depends on the available running time supplement [16].

It can be observed that the Hamiltonian is linear in the control u for both non-negative and negative control values, with coefficient $\lambda_2/v - 1$ for non-negative traction and λ_2/v for braking. Therefore, the optimal control structure can be split into five parts [16],

$$\hat{u}(s) = \begin{cases} u^{\max}(v(s)) & \text{if } \lambda_2(s) > v(s) & \text{(Maximum acceleration)} \\ r(v(s)) + g(s) & \text{if } \lambda_2(s) = v(s) & \text{(Cruising by partial traction)} \\ 0 & \text{if } 0 < \lambda_2(s) < v(s) & \text{(Coasting)} \\ r(v^{\max}(s)) + g(s) & \text{if } \lambda_2(s) = 0 & \text{(Cruising by partial braking)} \\ u^{\min}(v(s)) & \text{if } \lambda_2(s) < 0 & \text{(Maximal braking).} \end{cases} \tag{4.12}$$

The regime of cruising by partial traction corresponds to a unique optimal cruising speed v_c given as the implicit solution of [16]

$$v_c^2 r'(v_c) + \lambda_1 = 0. \tag{4.13}$$

The absolute value of $\lambda_1 < 0$ increases for shorter running time supplements, and therefore the optimal cruising speed is higher when less time supplement is available. In particular, the optimal cruising speed may be larger than the (local) speed limit depending on the specific conditions. Hence, the cruising speed by partial traction is given by $v(s) \equiv \min(v_c, v^{\max}(s))$, i.e., cruising at the speed limit is optimal for relative short time supplements. In contrast, cruising by partial braking only occurs at a speed limit $v^{\max}(s)$ during a downhill slope with gradient $g(s) \in \left[u^{\min} - r(v^{\max}), -r(v^{\max})\right]$ [16]. The cruising regimes may also be absent if the optimal cruising speed cannot be reached over relative short distances, depending on the stop distance and the speed limits.

The switching points in (4.12) depend on the co-state variable λ_2, which satisfies an adjoint ordinary differential equation defined by the negative partial derivative to speed of the Hamiltonian and the speed-dependent path constraints (4.4)–(4.5) [16],

$$\dot{\lambda}_2(s) = \frac{\lambda_1 + v\lambda_2 r'(v) + \lambda_2(u - r(v) - g(s))}{v^2} + \mu_1 u^+ + \mu_2, \tag{4.14}$$

where $\mu_1, \mu_2 \geq 0$ are Lagrange multipliers corresponding to the complementary slackness conditions of the path constraints $\mu_1(u^{\max}(v) - u) = 0$ and $\mu_2(v^{\max}(v) - v) = 0$, respectively. Hence, solving this optimal control problem requires solving a two-dimensional constrained boundary value problem of (v, λ_2) with boundary conditions $v(s_0) = v(s_1) = 0$ and none in λ_2, while depending on an implicit control function $u(v, \lambda_2)$ and an unknown cruising speed v_c (or λ_1). Algebraic formulae for the co-state λ_2 along track sections with constant gradient can be derived, which can be used to design efficient algorithms [1, 2, 18, 20]. In addition, constructive heuristic methods have been applied using the implicit knowledge of the optimal control structure (4.12). These solution methods are indirect methods in the sense that they are based on solving the derived optimality conditions from the Pontryagin's Maximum Principle. An alternative is given by direct solution methods that transcribe the continuous optimal control problem into a discrete nonlinear programming (NLP) problem by discretizing the state and control variables, the differential equations and the integral objective function. The resulting NLP problem can then be solved using efficient nonlinear optimization algorithms without a priori knowledge of the control structure [4]. In particular, pseudospectral methods have been developed for train trajectory optimization problems [16, 34, 37, 42]. The solutions so obtained can be checked to satisfy the optimality conditions, and in particular the optimal control structure (4.12) [16].

4.3.3 Illustrative Examples

This subsection illustrates the energy-efficient driving between two stops for several scenarios: long-distance versus short distance, the impact of a temporary speed restriction, and the effect of different running time supplements. The main results are summarized in Table 4.1.

Figure 4.3 from the previous section illustrates typical energy-efficient train trajectories for long and short distances. The static speed limit is 140 km/h in both cases. The applied running time supplements are 10% of the minimum running times. Figure 4.3 (left) shows the minimum-time (red) and the energy-optimal speed profile (blue) for a long distance train over a distance of 50 km. For the given running time supplement the optimal cruising speed is 132.2 km/h and the train starts coasting at 40.4 km, so that the train does not consume any traction energy in the last 9.6 km (19.2%). The coasting regime lasts for 325 s, which is 21.4% of the scheduled running time. Compared to the minimum time train control the energy-efficient train control thus applies a cruising speed below the speed limit and also has an additional coasting regime. The energy consumption reduces from 524.5 to 409.5 kWh, so that the energy-optimal driving strategy saves 21.9% energy with respect to the minimum running time.

Figure 4.3 (right) shows the minimum-time (red) and the energy-optimal speed profile (blue) for a local train over a short distance of 5 km. The optimal cruising speed is not reached within the distance and so the train accelerates to an optimal coasting point at 1.7 km reaching a maximal speed of 100.6 km/h after which the train starts coasting until the final braking regime. In this case, the train uses only maximal traction for the first part of the train run and then no longer requires traction energy for the remaining 3.3 km (66%). Note that also the minimum-time driving strategy cannot reach the speed limit within this distance and therefore accelerates to a speed of 129.3 km/h after which it already has to start braking to come to a standstill at the stop. The energy consumption reduces from 108.6 to 58.4 kWh, which is an energy saving of 46.3%.

Figure 4.4 (left) illustrates the energy-efficient speed profile for a long-distance train for various running time supplements, on a 50 km long track with a speed restriction of 125 km/h between 25 and 30 km. We here show both the impact of a speed restriction and varying running time supplements. Due to the speed restriction the minimum running time is 18 s longer than the long-distance case above without the speed restriction, since the train has to slow down its speed by 15 km/h during the speed restriction. The reduced speed and the reacceleration after the speed restriction leads to an increase in energy consumption of 12.7 kWh (2.4%) to 537.2 kWh for the minimum running time. The running time supplements are computed regarding this minimum running time.

In the case of 10% supplement, the optimal cruising speed is higher than the speed restriction and therefore the train has to reduce speed for this speed restriction. The optimal driving strategy now includes two coasting regimes, one before the speed restriction and one before the final braking at the end before the stop. At both sides

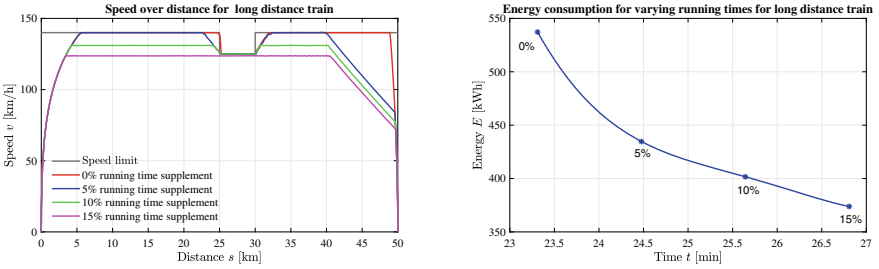

Fig. 4.4 The impact of a speed restriction (125 km/h) and varying running time supplements to a long-distance train: (left) speed-distance diagram for varying running time supplements and (right) the energy over running time diagram

of the speed restriction the train has a cruising regime with the same optimal cruising speed of 131.0 km/h, while during the speed restriction the train cruises at the lower restricted speed limit of 125 km/h. The switching points for both coasting regimes are determined implicitly by the unique cruising speed for the available running time supplement. The train re-accelerates with maximal tractive effort back to the optimal cruising speed after the train rear passed the speed restriction. With the 5% running time supplement the optimal cruising speed of 140.5 km/h exceeds the speed limit so that in this case the speed limits are applied in all cruising regimes. The difference with the minimum-time running is in this case only the coasting regimes before the speed restriction and before the stop. With 15% supplement the optimal cruising speed is 123.7 km/h, which is lower than the speed restriction so that in this case the restricted speed has no effect and the optimal driving strategy reduces to a single cruising and coasting regime like in the case of no speed restriction.

Figure 4.4 (right) illustrates the traction energy consumption as function of running time (supplement). When the amount of running time supplement increases the energy consumption goes down. In general, adding supplement in the beginning leads to more energy saving than increasing the supplement by the same amount later. Note that the last point corresponding to a train run with 15% running time supplement does not suffer from the energy loss due to the speed restriction, and therefore the energy saving with respect to the 10% point is more than from 5% to 10% in which cases the train has to reaccelerate after the speed restriction consuming extra energy.

It can be observed that much energy can be saved by adding even some small running time supplement percentage, as opposed to scheduling at the minimum running time. Likewise, a train will use much more energy when it runs as fast as possible in an attempt to recover a delay. Therefore, instead of running as fast as possible until a delay has been recovered, an energy-efficient delay recovery driving strategy is to recompute the optimal train trajectory for the remaining available running time supplement [35]. For instance, if the train scheduled with 10% supplement from Fig. 4.4 has a departure delay of 70 s then this reduces the remaining running time supplement from 10% to 5%. The optimal driving strategy then will change to the

one corresponding to 5% running time supplement which will provide an on-time arrival time with the least energy consumption. Hence, in this case the optimal cruising speed will be increased to the speed limits and the coasting points start a bit earlier. The energy consumption will then increase by 33.1 kWh (8.2%) from 401.6 to 434.7 kWh.

4.4 Energy-Efficient Train Timetabling Over Multiple Stops

4.4.1 Problem Formulation

The previous section considered the problem of finding the energy-efficient train trajectory between two stops for a given scheduled running time. When designing a train schedule over a line with multiple stops, the total scheduled running time over the line may be given while the allocation of the running time supplements between the successive stops may still be optimized. This is in particular relevant for stops without sidings on a railway line between multi-platform stations where trains may meet and overtake. The total running time between the stations then consists of train runs over one or more stops plus the dwell times at the intermediate stops. A scheduling approach often used in practice is to consider each train run between two adjacent stops separately and allocating the same percentage of running time supplement to these segments.

In this section we consider the multi-stop energy-efficient train trajectory optimization problem. The aim is find the optimal distribution of running time supplements between successive stops of a single train in a corridor for a given total scheduled running time T, such that the total traction energy of the train trajectory over the entire line is minimized. This problem is an extension of the energy-efficient train control problem between two stops. It can also be viewed as an optimal scheduling problem that finds the optimal arrival and departure times at intermediate stops such that the total energy consumption of the train trajectories in the corridor is minimized for a given total scheduled running time T.

The (multi-stop) energy-efficient train trajectory scheduling problem aims to minimize the total traction energy of the train trajectory of a train over a corridor with n segments over given stop positions $(s_0, \ldots, s_n)$ with a total scheduled running time T. The optimal control problem is then given as

$$\text{Minimize} \int_{s_0}^{s_n} u^+(s)ds \tag{4.15}$$

under the constraints (4.2)–(4.5) and the boundary (and internal) conditions

$$t(s_0) = 0,\ t(s_n) = T,\ v(s_k) = 0, \quad k = 0, \ldots, n. \tag{4.16}$$

Note that the only difference with the EETC problem formulation from Sect. 4.3 is the extra stops (zero speed) at the $n-1$ intermediate positions $s_1, \ldots, s_{n_1}$, while the internal times $t(s_k)$ are free for these intermediate stops. The multi-stop train trajectory optimization will therefore also determine the optimal intermediate arrival times $t(s_k)$. Note that the dwell times at the stops have been discarded, so the total running time T has been reduced by the sum of intermediate dwell times, which can be added to the stops after the optimization of the running times. The dwell times can also be included explicitly by defining free arrival and departure times at each stop that are connected by a fixed given dwell time in between [35, 36].

4.4.2 Optimality Conditions

The necessary optimality conditions are exactly the same as the solution of the two-stop case given in Sect. 4.3.2, i.e., the optimal control structure (4.12) still holds for the multi-stop case, including the implicit expression of the optimal cruising speed (4.13) and the dynamic equation (4.14) for the co-state λ_2 [30]. In particular, it can be proved that the optimal cruising speed is unique over the entire line when the arrival and departure times of intermediate stops are not constrained by restricted time windows [17]. Note that this problem is a special case of the train trajectory optimization problem between two stops with fixed scheduled running time, where the speed bound constraint (4.4) includes zero upper bounds at discrete intermediate points. As was illustrated in Fig. 4.4, the optimal cruising speed was uniquely determined by (4.13) resulting in an equal cruising speed at both sides of a speed restriction. The knowledge that the optimal cruising speed is unique over a corridor can be used for designing efficient algorithms [17, 30].

Of course, the internal boundary conditions force the train trajectory to zero speed at the intermediate stop positions, by which the speed profile looks like several train trajectories over successive stops. However, these train trajectories are dependent in the sense that the overall running time supplement is optimally distributed between all stops. This causes the same optimal cruising speed on each segment of the corridor and also determines the exact switching points between the driving regimes on each of them.

If an intermediate stop has a fixed target arrival or departure time, then the problem is split into two separate train trajectory optimization problems with the fixed event time at this stop as the final condition for the first problem and as initial condition for the second problem. This will reduce the flexibility of the optimization and thus result in a larger total energy consumption over the corridor. In particular, when the times at all intermediate stops are scheduled in advance before the train trajectory optimization then the energy consumption can only be optimized for the fixed sched-

uled running times between successive stops. The optimal scheduling method from this section, on the other hand, would exchange running time supplements between segments such that any supplement is added where needed the most.

4.4.3 Illustrative Example

This section illustrates the energy-efficient trajectory optimization and scheduling strategies over multiple stops with a case study for an intercity (IC) train from Utrecht Central (Ut) to Arnhem Central (Ah) in the Netherlands, with three intermediate stops in Driebergen-Zeist (Db), Veendendaal-De Klomp (Klp) and Ede-Wageningen (Ed). The speed limit is 140 km/h and the total distance is 60 km, with the intermediate stops at 10, 33 and 40 km. So this line has two shorter station distances of 10 and 7 km, and two longer station distances of 23 and 20 km. The minimum running time is computed as 1930.4 s, consisting of the successive minimum running times 354.0 s (Ut-Db), 688.3 s (Db-Klp), 276.9 s (Klp-Ed) and 611.2 s (Ed-Ah). The total running time supplement over Ut–Ah is assumed to be 15%, i.e., 290 s, resulting in a scheduled running time of 2120 s (excluding the dwell times at the stops). Note that nowadays timetables in the Netherlands are calculated with a precision of 1/10 min.

The minimum-time and energy-efficient scheduling strategies are compared to other scheduling strategies that are often used in practice. In total, this section considers the following five scheduling strategies over multiple stops:

1. Minimum-time train trajectory,
2. Energy-efficient train trajectory with optimal distribution of supplements,
3. Uniform schedule with equal percentage of running time supplement (15%),
4. Tightened schedule with most supplement added to the end,
5. Actual schedule with oscillating supplement percentages.

Table 4.1 summarizes the main results of these strategies, while Table 4.2 shows the optimal running time distribution and the maximum speed for each segment.

First, we focus on the energy-efficient train trajectories. Figure 4.5 (left-top) shows the energy-efficient speed profiles (in green). The 2nd and 4th long segments show identical optimal cruising speeds of 131.2 km/h, while the coasting starts later for the longer 2nd segment. The 1st and 3rd short segments are too short to reach the optimal cruising speed and therefore the train accelerates to an optimal coasting point with associated coasting speed after which it starts coasting. The coasting speed depends on the stop distance and is higher for the longer 1st segment where switching occurs at speed 118.8 km/h, while on the 3rd segment switching to coasting occurs at a speed of 104.0 km/h.

Figure 4.5 (right-bottom) shows the optimal relative running time supplements in percentage of the associated running times, which are deceasing for longer stop distance. Hence, when distributing a fixed amount of running time supplement over a schedule with multiple stops, allocating relative more running time supplement to shorter distances will lead to more energy saving than a uniform distribution. For

Table 4.1 Main results of the different scenarios

Scenario	Figures	Running time [s]	Supplement [%]	Energy [kWh]	Energy saving [%]
MTTC long distance	4.3	1380.7	0	524.5	–
EETC long distance	4.3	1518.8	10.0	409.5	21.9
MTTC short distance	4.3	222.1	0	108.6	–
EETC short distance	4.3	244.3	10.0	58.4	46.3
MTTC speed restriction	4.4	1398.7	0	537.2	–
EETC 5% supplement	4.4	1468.6	5.0	434.7	19.1
EETC 10% supplement	4.4	1538.5	10.0	401.6	25.2
EETC 15% supplement	4.4	1608.5	15.0	373.8	30.4
MTTC Ut–Ah	4.5	1930.4	0	602.1	–
EETC Ut–Ah tightening	4.5	2120.0	15.0	400.0	33.6
EETC Ut–Ah uniform	4.5	2120.0	15.0	365.6	39.3
ETTC Ut–Ah practice	4.5	2120.0	15.0	391.4	35.0
ETTC Ut–Ah optimal	4.5	2120.0	15.0	364.7	39.4

Legend MTTC = mimimum time train control, EETC = energy-efficient train control

Table 4.2 Running time supplements and maximum speed on the successive segments over the line Ut-Ah for five scheduling strategies

Segment	Ut–Db	Db–Klp	Klp–Ed	Ed–Ah
Supplement [s, %]				
MTTC	0 (0%)	0 (0%)	0 (0%)	0 (0%)
ETTC tightening	17.7 (5.0%)	34.4 (5.0%)	13.8 (5.0%)	223.6 (36.6%)
EETC uniform	53.1 (15.0%)	103.2 (15.0%)	41.5 (15.0%)	91.7 (15.0%)
EETC practice	152.8 (43.2%)	55.9 (8.1%)	69.6 (25.1%)	11.2 (1.8%)
EETC optimal	64.9 (18.3%)	89.2 (13.0%)	50.9 (18.4%)	84.6 (13.8%)
Maximal speed [km/h]				
MTTC	140.0	140.0	139.2	140.0
ETTC tightening	134.2	140.0	121.4	102.8
EETC uniform	122.0	128.1	107.7	129.0
EETC practice	96.5	140.0	98.5	140.0
EETC optimal	118.8	131.2	104.0	131.2

instance, the running time supplement over the shortest distance of 7 km (Klp–Ed) is 18.4% (51 s), while this is 13.0% (89.2 s) for the longest distance of 23 km (Db–Klp). Note that in terms of absolute running time supplements, those for the longer distance still may be longer, see Table 4.2. Overall, the energy-optimal train trajectory and schedule over the corridor with 15% total running time supplement saves 237.4 kWh (39.4%) energy consumption with respect to the minimum running time.

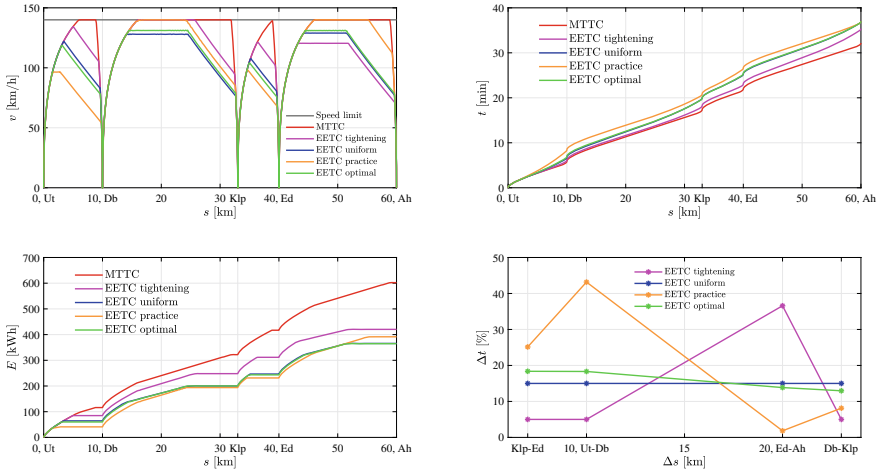

Fig. 4.5 Train trajectories for a train over multiple stops (Ut, Db, Klp, Ed, and Ah) for various driving strategies (minimum time, energy-optimal, uniform, tightening, practice): (left-top) speed-distance, (right-top) time-distance, (left-bottom) energy-distance, and (right-bottom) relative running time supplement over distance

Figure 4.5 also compares the results for the various scheduling strategies used in practice. The uniform schedule illustrates the deviation of the energy-optimal train trajectory from a uniform supplement percentage of 15%, i.e., providing a smaller supplement at the short stop distances and a larger one at the long stop distances. In the uniform case, the cruising speeds over the longer distances are lower than the optimal cruising speed corresponding to the longer running times on these segments, and they also vary with a lower cruising speed for the longer distance, 128.5 km/h on Db–Klp (23 km) and 130 km/h on Ed-Ah (20 km). On the short distances the maximal speeds obtained before coasting are higher than the optimal ones due to the shorter running times, 122 km/h on the 1st segment and 108 km/h on the 3rd. Still the increase in total energy consumption is negligible with less than 1 kWh (0.24%).

The tightened schedule was used in the period 2008–2015 in the Netherlands with the aim to obtain more robust schedules in the sense that the majority of the running time supplement is allocated before stations where punctuality is measured, which in this case is on the last segment of the corridor before Arnhem Central. Then, a delay on any of the segments on the corridor can be recovered as much as possible as opposed to 'wasted' supplements at the early segments when a delay occurs at the later segments. In this case, the first three segments still obtained (the minimum required) 5.0% running time supplement, while 36.6% is allocated at the last segment, see Table 4.2. As a result the maximal speeds obtained before coasting at the 1st and 3rd short distance segments are much higher then the optimal coasting speeds, and in the 2nd segment the train cruises at the speed limit of 140 km/h. In contrast, the cruising speed in the last segment is much lower with only 102.8 km/h. As a result, much energy is lost over specifically the two short distances and this

can hardly be compensated by the excessive supplement on the last long distance segment. This strategy uses 35.3 kWh (9.7%) more energy than the optimal strategy.

The current actual schedule (no longer designed according to the tightened strategy) uses significantly higher percentages at the short distances of 43.2% and 25.1% at Ut–Db and Klp–Ed, respectively, and lower percentages at the long distances of 8.1% on Db–Klp and only 1.8% on Ed–Ah. The planners added extra running time supplement before Db and Ed, at the cost of the supplement before Klp and in particular Ah. As a result the reached speeds at the short distances are lower with longer coasting regimes, while on Ut-Db even a short cruising regime at 96.5 km/h occurs to avoid that the speed becomes too slow at the end of the coasting regime. On the long distances cruising at the speed limit is applied with in particular only a short coasting regime on the last long distance segment. In this case, the additional energy consumption on the corridor is 26.7 kWh (7.3%).

4.5 Energy-Efficient Timetabling of Multiple Trains Over a Corridor

4.5.1 Problem Formulation

Unnecessary loss of energy occurs if a train must brake due to a conflicting preceding train and then needs to re-accelerate when the route ahead is available again. Not only does the re-acceleration cause additional energy consumption compared to a conflict-free train run, but the train also has to run faster to compensate for the delay caused by the unplanned braking and possible waiting before a signal until the train is allowed to proceed again. Train path conflicts may be caused by inaccurate timetabling or by schedule deviations during operations either by a delayed preceding train or by early running, when two trains want to occupy a shared track at the same time. In practice the railway signalling systems will intervene by which one of the two trains will have to slow down. This train will then be delayed and allocate tracks for a longer time than scheduled, which may cause a further cascade of path conflicts and delays to later trains in case of heavily occupied networks.

The railway timetable therefore must provide conflict-free train paths such that each train should be able to run according to its scheduled train trajectory without route occupation conflicts. This is also called a green wave in the sense that the trains will not meet restricted signals due to conflicting trains if they all adhere to their schedule [8, 34]. In addition, a railway timetable must be robust in the sense that it should contain some buffer time between successive train paths such that a slight deviation from the schedule will not immediately lead to a route occupation conflict [15]. In the case of bigger disturbances traffic management must detect possible conflicts and resolve them proactively to maintain a conflict-free traffic plan to avoid a waste of energy and track capacity [25].

In the previous sections the focus was on scheduling a single train trajectory between stops or over corridors. From the infrastructure perspective, the train trajectory allocates the track sections on a route exclusively to a train over certain time slots during which they are blocked to other trains. These blocking times depend on the speed profile of a train and the signalling system applied that guarantees safe train separation. In general, the railway infrastructure is partitioned into block sections that may contain only one train at a time. The signalling system dictates at which location a brake indication has to be given when approaching an occupied block. For conflict-free train running the block should be clear before reaching the brake indication point to that block. Otherwise, the train has to brake and thus deviate from its planned train trajectory.

Blocking times are computed using blocking time theory [22, 23]. The blocking time for a given block consists of the sum of six time components: the setup time, sight and reaction time, approach time, running time, clearing time, and release time. The setup time is the required time to set and lock the route in the block. The sight and reaction time represents the required time to respond to a brake indication in case of a restricted movement authority. The approach time models the running time over the approach distance from the brake indication point to the actual block. The running time is the time within the block. The clearing time is the running time over the train length at the end of the block until the complete train has left the block. And finally, the release time is the time to release the route and signals to be used by the next train. The approach, running and clearing time depend on the train speed and therefore the train trajectory, while the other three time components are often defined as time parameters conditional on the given infrastructure conditions.

Figure 4.6 illustrates the blocking time components for a single block section of a running train under three-aspect two-block signalling, where lineside signals indicate the movement authority using three aspects: stop (red) indicating that the train should stop before the block, approach (yellow) dictating to reduce speed and prepare to stop before the next signal, and clear (green) meaning that the train can proceed with the track speed [14]. In this case the brake indication is thus given by the approach signal. If the route in a block includes switches then all sections in the block are locked simultaneously but they may be released in parts to allow the switches to be set for another route, which is called the sectional-release route-locking principle, see the blocks between the 2nd and 3rd signal in Fig. 4.7. Note that the blocking time exceeds the physical occupation time of the block due the signalling constraints that require a train to start braking when it approaches a closed block and additional system times to set up and release the route.

Blocking times enrich the traditional time-distance diagrams by including the time slots that the successive blocks are blocked for a specific train path to allow conflict-free operation. With this additional information the infrastructure occupation of a train path operating under fixed-block signalling takes the form of a blocking time stairway, see Fig. 4.7. A conflict-free timetable should contain ‘white space’ between the blocking times of all successive trains. As a result, conflicts are now easily visualised by overlapping blocking times, which indicate that a train needs to reserve a block while it has not yet been released by the previous train, see Fig. 4.7

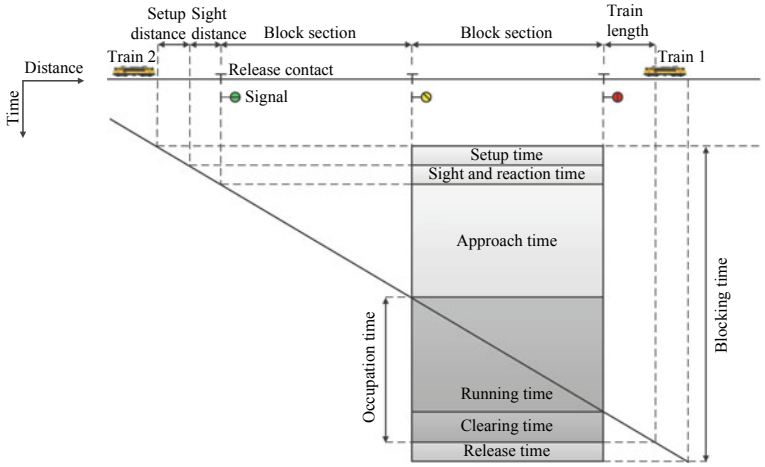

Fig. 4.6 Blocking time components

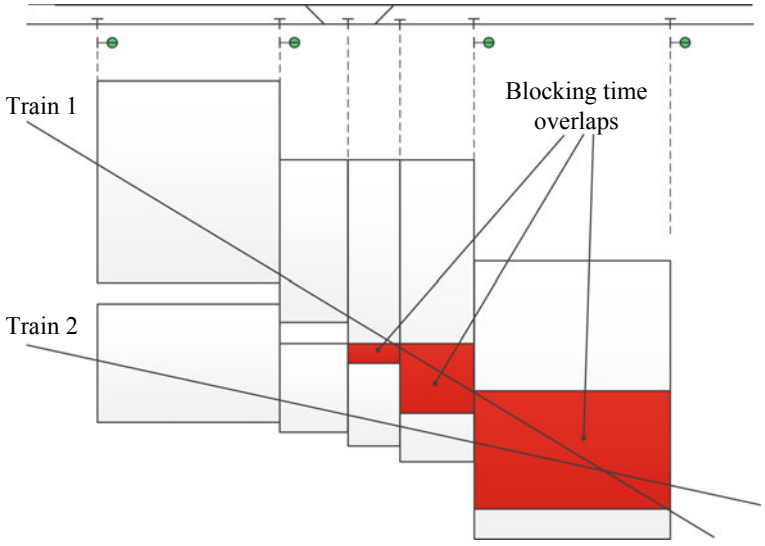

Fig. 4.7 Conflict detection by overlapping blocking time stairways

where two successive train paths are conflicting in the last two blocks. In addition, by compressing the blocking time stairways over a corridor the minimum line headway times can be calculated corresponding to critical blocks between the successive train paths where adjacent blocking times are touching each other. If the scheduled train paths respect these minimum headway times at the line level then they will be conflict-free, including any running time differences between successive trains for heterogeneous traffic. A conflict-free timetable should include some buffer time on

top of the minimum line headway times to be robust to small train path deviations. The compressed blocking time stairways of all train paths scheduled in a given time period without any buffer time at the critical blocks give the infrastructure occupation of the associated timetable structure, which is a measure of the used capacity [15].

In the following, we assume that the desired scheduled departure and arrival time at respectively the first and last station of a corridor are given, and hence also the scheduled running time for each train on the corridor. The problem is then an extension to the one from the previous section to find the energy-efficient train trajectories of all trains over the corridor such that they do not have conflicting infrastructure occupation. This problem can be modelled as a multi-train trajectory optimization problem [35, 36], where the event times of m successive trains at certain positions are restricted by minimum headway times, as follows.

Let n_i be the number of successive train runs of train $i \in \{1, \ldots, m\}$ and $s_{ik} \in S_i = \{s_{i0}, \ldots, s_{in_i}\}$ the stop positions of train i. Note that the trains may have different stop positions. Denote common locations of two successive trains i and j (in this order) that require a headway constraint by $(s_{ik}, s_{jl}) \in S_{ij} \subseteq S_i \times S_j$ for $i \neq j$ with corresponding headway time h_{ikjl}. The timing points for headway constraints can also be generalized to fixed locations other than the stop positions, such as signal positions or station locations for non-stopping trains. The state and control variables as well as the resistance, speed and gradient profiles and other parameters for a train i are indicated with an index i. Finally, for each train i the scheduled departure time d_i at the initial stop position s_{i0} and the scheduled arrival time a_i at the final stop position s_{in_i} is given. Then the multi-train trajectory optimization problem can be defined as

$$\text{Minimize} \sum_{i=1}^{m} \int_{s_{i0}}^{s_{in_i}} u_i^+(s) ds \tag{4.17}$$

subject to the following constraints for all trains $i \in \{1, \ldots, m\}$,

$$\dot{t}_i(s) = 1/v_i(s) \tag{4.18}$$

$$\dot{v}_i(s) = (u_i(s) - r_i(v) - g_i(s))/v_i(s) \tag{4.19}$$

$$0 \leq v_i(s) \leq v_i^{\max}(s) \tag{4.20}$$

$$u_i^{\min}(v_i) \leq u_i(s) \leq u_i^{\max}(v_i), \tag{4.21}$$

the boundary and internal conditions

$$t_i(s_{i0}) = d_i,\ t_i(s_{in_i}) = a_i,\ v_i(s_{ik}) = 0, \quad s_{ik} \in S_i, \tag{4.22}$$

and the pairwise headway time constraints linking the train trajectories at fixed locations

$$t_j(s_{jl}) - t_i(s_{ik}) \geq h_{ikjl}, \quad (s_{ik}, s_{jl}) \in S_{ij}, \tag{4.23}$$

for all trains $i, j \in \{1, \ldots, m\}$. Recall that we considered fixed event times at the beginning and end of the corridor and so also the sequence orders are fixed between the trains over the corridor including possible order changes at overtaking locations. In a more general timetable optimization problem the order may still have to be decided which will complicate the headway constraints (4.23).

Note that trains can take different routes, so that formally the independent variable s can be different for each train i, and therefore also the gradient $g_i(s)$ and speed limits $v_i^{\max}(s)$ depend on train i. For the modelling of different routes using multiple-phase optimal control, see Wang and Goverde [35, 36].

4.5.2 Solution Procedure

The necessary optimality conditions from Sect. 4.4 are still valid for each train trajectory in the multi-train multi-stop train trajectory optimization problem, and in particular the optimal control structure (4.12) still holds with a unique cruising speed per train over the entire corridor. The headway time constraints between the time-distance paths of pairs of trains at fixed locations provide additional timing constraints that depend on both train trajectories, as opposed to simple fixed timing or speed constraints for single train trajectories. If the inequalities (4.23) are not active then all trains will be able to run according to the energy-efficient single-train trajectories. Only in case of conflicts the headway time constraints become active and the train trajectories have to be jointly optimized to satisfy these constraints.

The general procedure to find energy-efficient train trajectories of multiple trains over a corridor can be given as follows [35, 36]:

1. Solve the energy-efficient train trajectory optimization problem (over two or more stops) for each train in the corridor for fixed departure and arrival time at the corridor ends.
2. Compute the corresponding blocking time stairways for all trains and check for overlapping blocking times (i.e., conflicts).
3. Resolve the conflicts by a multi-train trajectory optimization problem over the conflicting trains considering headway constraints.

We can distinguish three different situations for scheduling trains over a corridor:

- Double-track lines with one running direction per track,
- Double-track lines with one running direction per track and intermediate overtaking stations or sidings,
- (Partially) single-track lines with opposite trains meeting at passing stations or sidings.

Also combinations are possible with in particular multiple-track lines, and two railway lines may merge at a junction so that trains from different lines are combined on the track after the junction, or in the opposite direction, successive trains can divert into different directions after a diverging junction. The basic principles still apply to these situations.

If the interval between successive scheduled departure times at the origin station of a corridor exceeds the minimum line headway times then the associated blocking time stairways will not overlap and the train trajectories will be conflict-free. An exception occurs if the railway line allows overtakings (the 2nd situation) or meetings between opposite trains (the 3rd situation), in which cases the train trajectories must be synchronized at the meeting or overtaking points.

Since railway timetabling is an NP-hard problem, Goverde et al. [15] proposed a three-level framework where first a conflict-free timetable on the network level is computed using a micro-macro iterative approach, after which energy-efficient train trajectories are embedded over the corridors. The microscopic level computes the running and blocking times and checks for conflicts and acceptable infrastructure occupation using blocking time theory, while the macroscopic level optimizes the event times at the main stations considering optimal and robust travel times [5]. Then at the third fine-tuning level the corridors between the main stations are optimized for fixed target times at the corridor ends using train trajectory optimization. First, the non-stop intercity train trajectories are computed using the train trajectory optimization problem over the entire corridor, like the model from Sect. 4.3. For the local train trajectories over the corridors, the impact of stochastic intermediate dwell times were considered using a stochastic model formulated as a multi-stage multi-criteria decision problem that was solved by dynamic programming. The model from the current section is an alternative approach to solve the energy-efficient timetable problem over the corridors. Moreover, this model can also be embedded at the microscopic level. The third level can then be discarded unless the stochastic dwell times should be considered. A simpler rapid running time calculation model was developed for the microscopic level that determined the timetable (cruising) speed to cover the scheduled running time without considering coasting. Since in this iterative framework train trajectories have to be (re)computed for many lines over a large-scale network rapid computation time is crucial.

4.5.3 Illustrative Examples

In this section we provide two examples corresponding to the situations of a double-track line [28] and a double-track line with an overtaking [36]. For the case of single-track lines, see Wang and Goverde [35, 36].

The first case study considers the Dutch corridor of about 18.5 km between the main stations Arnhem Central (Ah) and Nijmegen (Nm), with the intermediate stations Arnhem Zuid (Ahz), Elst (Est) and Nijmegen Lent (Nml). A long-distance intercity (IC) train only stops at the main stations Ah and Nm, while the short-distance regional (RE) train stops at all stations with 42 s dwell time. Both train types share the same route over the corridor, except at the first and last block section due to different track and platform use at Ah and Nm, so we do not consider overtaking on the railway line between these stations. For details of the rolling stock characteristics, blocking time parameters, and the track characteristics such as gradients, speed limits and signal positions, see Scheepmaker and Goverde [28].

The aim of this case study is to find an energy-efficient timetable for alternating intercity and regional trains from Ah to Nm that repeat at a regular interval of 15 min, so with a frequency of 2×4 trains per hour. A minimum running time supplement of 8% is required for both trains, and a minimum buffer time of 30 s must be included over the minimum line headway time between the trains. The quality of the timetable can be measured by four indicators: total scheduled running time (including intermediate dwell times) and energy consumption of both train types, the infrastructure occupation, and the total buffer time. Larger running times imply lower energy consumption, because more supplement is available for energy-efficient driving. On the other hand, the infrastructure occupation depends on the running time difference between the IC and RE trains, and therefore on the relative allocation of running time supplement to the two trains over this corridor. Finally, higher infrastructure occupation means less buffer time and therefore a lower stability regarding delays. The infrastructure occupation can be minimized by homogenizing the two trains, i.e., slow down the IC trains by adding a large running time supplement, or speeding up the RE trains by including only the minimum supplement. However, this will have a negative affect on the running time for the IC train or on the energy consumption of the RE train. An optimal solution can be found by considering a multi-objective optimization problem, and in particular a weighted sum of the four indicators [28]. The optimal solution allocates 12% running time supplement to the IC train and 9.5% to the RE train. The total buffer time is 4 min and the infrastructure occupation is 73.3%. Figure 4.8 illustrates the compressed blocking time diagram for the energy-efficient driving strategies. The shown blocking times are extended with the 30 s required minimum buffer time (dark areas). The minimum line headway time is 156 + 30 s minimum buffer time from the IC to the RE train, and 504 + 30 s from the RE to the IC train. A regular interval timetable can be obtained by dividing the extra 180 s buffer time between the train pairs, such that the second IC train departs at 15 min (in the next cycle). Possible departure times from Ah could then be the IC at 0 s and the RE at 240 s repeating every 15 min (900 s), with resulting buffer times of 94 s and 156 s, respectively.

The second case study considers the 50 km long Dutch corridor between the main stations ‘s-Hertogensbosch (Ht) and Utrecht Central (Ut), with six intermediate stations Zaltbommel (Zbm), Geldermalsen (Gdm), Culemborg (Cl), Houten Castellum (Htnc), Houten (Htn), and Utrecht Lunetten (Utl). Gdm is an overtaking station. The considered periodic timetable includes four trains per 30 min: two IC trains stopping only in Ht and Ut, one RE train from Ht to Ut that is overtaken by an IC train at Gdm, and another RE train that merges into the corridor at Gdm and runs to Ut after the other IC train. The scheduled departure and arrival times at the start and end stations are given and so are the original arrival and departure times at all intermediate stops for the RE trains, see Table 4.3. Note that the trains of equal type do not follow a strict departure interval of 15 min, but a 14–16 min interval. In the longer interval additional freight paths can be operated, which are not considered here. The dwell times on the short stops of the RE trains should be within 30 and 60 s, and at the overtaking station Gdm between 180 and 360 s. For an overtaking a default headway time of 120 s applies both between arrival of the stopping train and the passing IC

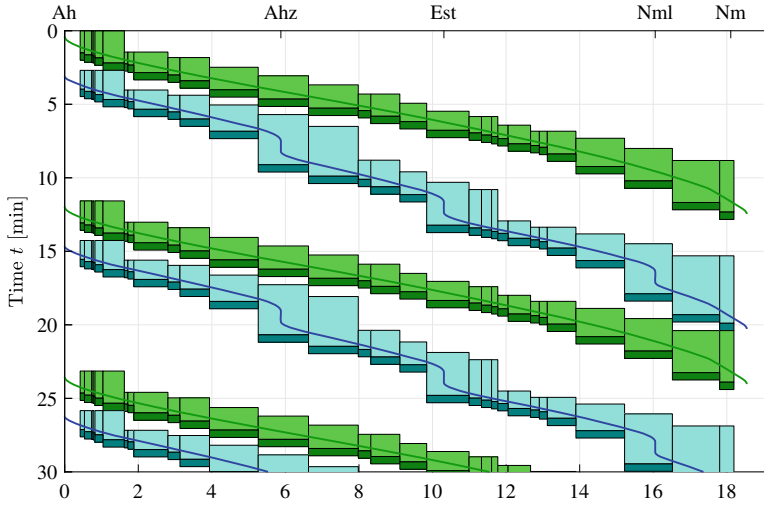

Fig. 4.8 Compressed blocking time diagram with energy-efficient train trajectories for optimized running time supplements of an IC (green) and RE train (blue)

train, and from the passing IC train to the departure of the stopping train. For details about the rolling stock and track characteristics, see Wang and Goverde [36].

The aim of this case study is to find an energy-efficient timetable over the corridor for the four trains per hour, while the start and end times are fixed. The results are summarized in Table 4.3. Figure 4.9 (left) illustrates the results of the train trajectory optimization for all four trains separately, with the corresponding blocking times. The two IC trains show the energy-efficient train trajectory between two stops, which are the same as both have the same scheduled running time of 28 min. The train trajectory optimization of the RE trains includes optimization of the arrival and departure times at the intermediate stops, see Table 4.3. In particular, the 2nd RE train running from Ht to Ut arrives 1 min later at Gdm compared to the original timetable and departs 1 min earlier, thus reducing the dwell time at Gdm from 5 to 3 min. Therefore, also the remaining running time from Gdm to Ut increases from 15 to 16 min, by which the train trajectory of this RE train is different from the one that starts from Gdm at the original fixed departure time. The energy saving is 21.8% for the RE train Ht-Ut and 17.3% for the other RE train Gdm-Ut compared to the energy-efficient train trajectories that can be obtained while sticking to the original timetable at the intermediate stops. The energy consumption of the IC trains in the original timetable is also computed for the energy-efficient train trajectories, although the original speed profiles were probably different.

Figure 4.9 (left) shows overlapping blocking time stairways after Gdm between the RE train and the IC train that should overtake this RE train at Gdm (the red blocking times). Since the dwell time of the RE train is now 3 min, it does not satisfy the default headway times of 2 min before and after passage by the IC. Therefore, we apply a multi-train trajectory optimization for these two trains with additional headway constraints of 120 s at Gdm between the arrival time of the RE train and

Table 4.3 The original and optimized timetables for the double-track corridor Ht-Ut

Train	Event	Ht	Zbm	Gdm	Cl	Htnc	Htn	Utl	Ut	Energy [MJ]	Saving
Original timetable											
RE1	A	–	–	–	12:30	18:30	22:30	26:30	32:00	0.3966	–
	D	–	–	07:00	13:00	19:00	23:00	27:00	–		
RE2	A	–	11:30	18:00	28:30	34:30	38:30	42:30	48:00	0.7342	–
	D	02:00	12:00	23:00	29:00	35:00	39:00	43:00	–		
IC1	A	–	–	–	–	–	–	–	37:00	1.2394	–
	D	09:00	–	–	–	–	–	–	–		
IC2	A	–	–	–	–	–	–	–	51:00	1.2394	–
	D	23:00	–	–	–	–	–	–	–		
Single-train trajectory optimization											
RE1	A	–	–	–	13:00	20:00	22:48	27:18	32:00	0.3281	17.3%
	D	–	–	07:00	13:30	20:30	23:18	27:48	–		
RE2	A	–	11:42	19:00	28:30	36:00	38:48	43:12	48:00	0.5741	21.8%
	D	02:00	12:12	22:00	29:00	36:30	39:18	43:42	–		
IC1	A	–	–	–	–	–	–	–	37:00	1.2394	0%
	D	09:00	–	–	–	–	–	–	–		
IC2	A	–	–	–	–	–	–	–	51:00	1.2394	0%
	D	23:00	–	–	–	–	–	–	–		
Multi-train trajectory optimization											
RE2	A	–	12:00	20:00	30:00	36:42	39:30	43:00	48:00	0.6355	13.4%
	D	02:00	12:30	24:00	30:30	37:12	40:00	43:30	–		
IC1	A	–	–	–	–	–	–	–	37:00	1.2394	0%
	D	09:00	–	–	–	–	–	–	–		

A arrival time [mm:ss]; *D* departure time [mm:ss]

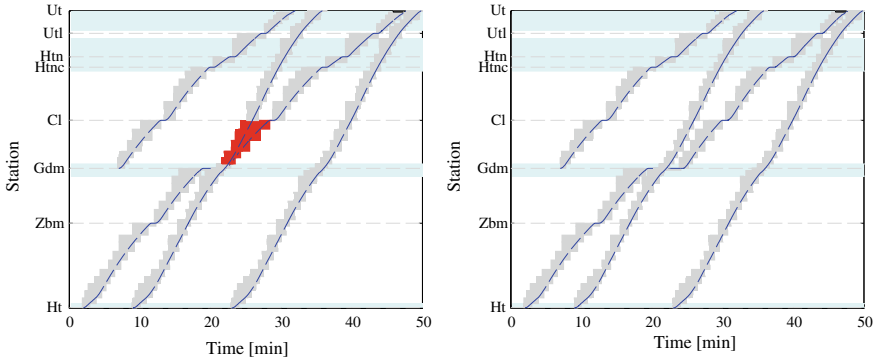

Fig. 4.9 Blocking time diagrams of energy-efficient train trajectories with conflict indicated by the red overlapping blocking times (left) and resolved conflict (right). *Source* [36]

the passage of the IC train, and likewise between the latter and the departure time of the RE train. The result is illustrated in Fig. 4.9 (right) that shows a conflict-free timetable. The arrival time of the RE train in Gdm is now another 1 min later and the departure time 2 min later, with the minimal dwell time of 4 min that is required by the two headway times. This will provide the maximal running time supplement for the RE over the corridor. The energy-efficient train trajectory of the IC train did not change, so that it was optimal to adjust the train trajectories from the RE train before and after the passage time of the IC train, which happens to be at 22 min in the basic half hour period. The energy saving of the RE train reduced to 13.4% to allow a conflict-free timetable.

Figure 4.10 illustrates the speed profiles of the various energy-efficient train trajectories. The speed profile for the IC train obtained from the single-train trajectory optimization (4th plot) is the same as the one obtained from the multi-train trajectory

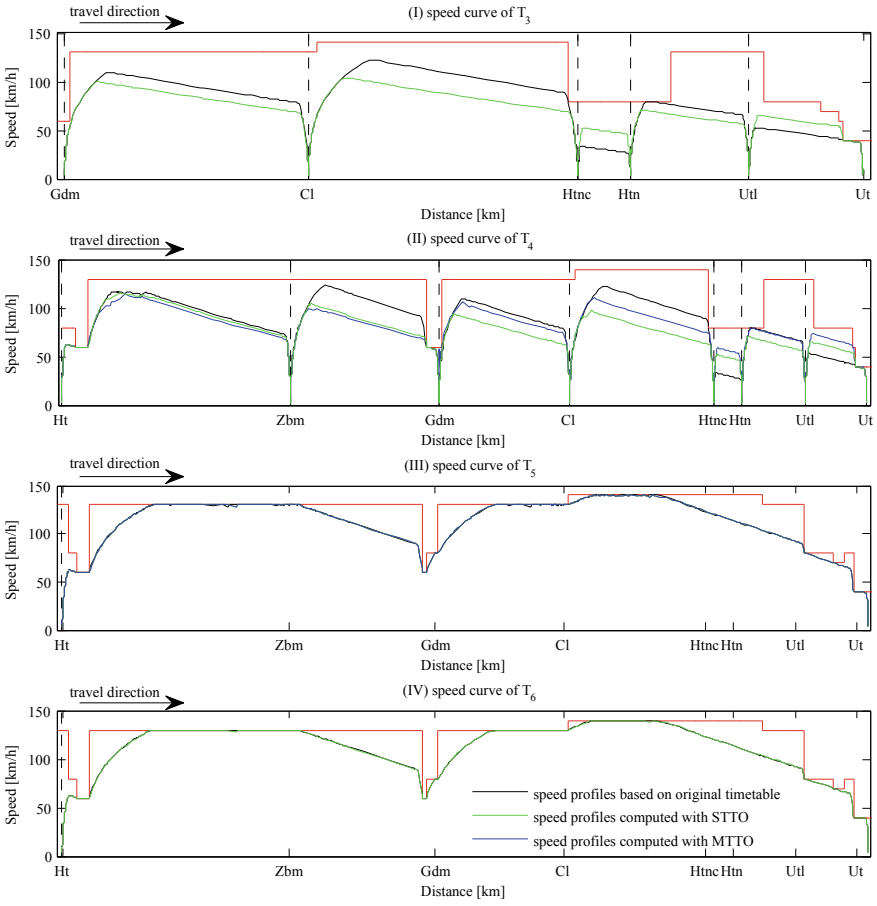

Fig. 4.10 Speed profiles for the trains on the double-track corridor Ht-Ut. *Source* [36]

optimization (3rd plot). For the RE train Ht-Ut (2nd plot) three different speed profiles can be observed. For the original timetable the speeds are higher before Gdm as the scheduled running time from Ht to Gdm is shorter than in the optimal timetables. The original scheduled running time over Gdm-Ut is 1 min larger than in the solution from the multi-train trajectory optimization. However, the latter optimizes the arrival and departure times at the intermediate stops, which results in a different allocation of the supplements between the various stops. The speeds of the optimized solution are still lower on the two longer runs Gdm-Cl and Cl-Htnc corresponding to 30 and 42 s more running time, while on the short stretches after Htnc they are higher than the very slow speeds resulting from the original timetable, corresponding to reduced running times by 72 s, 30 s, and 30 s. In particular, the running time over the short stretch from Htnc to Htn was reduced by 34%.

4.6 Conclusions

This chapter showed how energy-efficient train trajectory optimization can be incorporated in railway timetabling. In particular, the scheduled arrival and departure times at stations as well as passage times of non-stop trains at stations or other timing points should be based on realistic speed profiles that include the impact of the allocated running time supplement. Moreover, for saturated railway networks it is essential that the assumed driving behaviour in the running time calculations from the planning phase are consistent with the actual driving strategies in actual train operation. Otherwise, train path conflicts may arise during operation while the plan was 'proven' to be feasible.

Energy-efficient train operation must be supported by a railway timetable that allows for energy-efficient driving. This means that the running time supplements must be allocated between the successive stops in such a way that train operation can be energy-efficient, and no energy is lost by drivers who try to adhere to scheduled arrival times that are scheduled in a naive way. The latter may occur for instance by short stretches with relatively much running time (supplement) due to rounding to full minutes, or scheduling much supplement just before main stations to improve punctuality statistics. Scheduling in a higher precision than full minutes is recommended to provide improved information to drivers or Automatic Train Operation. For instance, since a few years the Netherlands Railways plan their timetable with a precision of a tenth of a minute.

The successive speed profiles should be predictable and drivable. Energy-efficient speed profiles have equal cruising speeds over successive train runs, as opposed to varying timetable speeds between timing points due to scheduling of event times that are not based on valid speed profiles, such as the typical timetabling practice based on minimum running times plus some percentage or fixed amount of running time supplement, and this rounded to full minutes. It is useless to provide training for drivers to run in an energy efficient way or to develop advanced algorithms for

Driver Advisory Systems or Automatic Train Operation, if the timetable prevents energy-efficient driving [26].

Moreover, timetables must be conflict-free and robust so that minor deviations from a train path do not immediately lead to conflicts and delay following trains, as this will also result in unnecessary braking and re-acceleration and therefore in loss of energy. Energy-efficient train timetabling thus also calls for a microscopic approach where the constraints from the signalling system are realistically modelled in blocking times and resulting infrastructure occupation, which enables conflict detection and resolution between the scheduled train trajectories to guarantee conflict-free timetables.

The mathematical models and algorithms are available to develop performance-based energy-efficient train timetabling, including microscopic train trajectory optimization and conflict detection and resolution [15]. In particular, energy-efficient train trajectory optimization should become the standard running time calculation method in any timetabling design tools.

References

1. Albrecht AR, Howlett PG, Pudney PJ, Vu X, Zhou P (2016) The key principles of optimal train control-part 1: formulation of the model, strategies of optimal type, evolutionary lines, location of optimal switching points. Transp Res Part B Methodol 94:482–508
2. Albrecht AR, Howlett PG, Pudney PJ, Vu X, Zhou P (2016) The key principles of optimal train control-part 2: existence of an optimal strategy, the local energy minimization principle, uniqueness, computational techniques. Transp Res Part B Methodol 94:509–538
3. Albrecht T, Oettich S (2002) A new integrated approach to dynamic schedule synchronization and energy-saving train control. In: Allen J, Hill RJ, Brebbia CA, Sciutto G, Sone S (eds) Computers in railways VIII. WIT Press, Southampton, UK, pp 847–856
4. Betts JT (2010) Practical methods for optimal control and estimation using nonlinear programming. Advances in design and control. SIAM, Philadelphia, PA, USA
5. Bešinović N, Goverde RMP, Quaglietta E, Roberti R (2016) An integrated micro-macro approach to robust railway timetabling. Transp Res Part B Methodol 87:14–32
6. Binder A, Albrecht T (2013) Timetable evaluation and optimization under consideration of the stochastical influence of the dwell times. In: Proceedings of the 3rd international conference on models and technologies for intelligent transportation systems, pp 471–481
7. Cacchiani V, Toth P (2012) Nominal and robust train timetabling problems. Euro J Oper Res 219(3):727–737
8. Corman F, D'Ariano A, Pacciarelli D, Pranzo M (2009) Evaluation of green wave policy in real-time railway traffic management. Transp Res Part C Emerg Technol 17(6):607–616
9. Cucala AP, Fernández A, Sicre C, Domínguez M (2012) Fuzzy optimal schedule of high speed train operation to minimize energy consumption with uncertain delays and driver's behavioral response. Eng Appl Artif Intell 25(8):1548–1557
10. Davis W (1926) The tractive resistance of electric locomotives and cars. Gen Electr Rev 29:685–707
11. Ghoseiri K, Szidarovszky F, Asgharpour MJ (2004) A multi-objective train scheduling model and solution. Transp Res Part B Methodol 38(10):927–952
12. González-Gil A, Palacin R, Batty P (2013) Sustainable urban rail systems: strategies and technologies for optimal management of regenerative braking energy. Energy Convers Manage 75:374–388

13. Goverde RMP, Hansen IA (2013) Performance indicators for railway timetables. In: 2013 IEEE international conference on intelligent rail transportation proceedings, pp 301–306
14. Goverde RMP, Corman F, D'Ariano A (2013) Railway line capacity consumption of different railway signalling systems under scheduled and disturbed conditions. J Rail Transp Plann Manage 3(3):78–94
15. Goverde RMP, Bešinović N, Binder A, Cacchiani V, Quaglietta E, Roberti R, Toth P (2016) A three-level framework for performance-based railway timetabling. Transp Res Part C Emerg Technol 67:62–83
16. Goverde RMP, Scheepmaker GM, Wang P (2021) Pseudospectral optimal train control. Euro J Oper Res 292:353–375
17. Howlett PG (2016) A new look at the rate of change of energy consumption with respect to journey time on an optimal train journey. Transp Res Part B Methodol 94:387–408
18. Howlett PG, Pudney PJ, Vu X (2009) Local energy minimization in optimal train control. Automatica 45(11):2692–2698
19. Huang K, Liao F, Gao Z (2021) An integrated model of energy-efficient timetabling of the urban rail transit system with multiple interconnected lines. Transp Res Part C Emerg Technol 129:103171
20. Liu RR, Golovitcher IM (2003) Energy-efficient operation of rail vehicles. Transp Res Part A Policy Pract 37(10):917–932
21. Lusby RM, Larsen J, Ehrgott M, Ryan D (2011) Railway track allocation: models and methods. OR Spectrum 33(4):843–883
22. Pachl J (2009) Railway operation and control. VTD Rail Publishing, Mountlake Terrace, WA, USA
23. Pachl J (2014) Timetable design principles. In: Hansen IA, Pachl J (eds) Railway timetabling and operations. Eurailpress, Hamburg, Germany, pp 13–46
24. Pontryagin LS, Boltyanskii VG, Gamkrelidze RV, Mishchenko EF (1962) The mathematical theory of optimal processes. Wiley, Hoboken, NY, USA
25. Quaglietta E, Pellegrini P, Goverde RMP, Albrecht T, Jaekel B, Marlière G, Rodriguez J, Dollevoet T, Ambrogio B, Carcasole D (2016) The ON-TIME real-time railway traffic management framework: a proof-of-concept using a scalable standardised data communication architecture. Transp Res Part C Emerg Technol 63:23–50
26. Scheepmaker GM, Goverde RMP (2015) The interplay between energy-efficient train control and scheduled running time supplements. J Rail Transp Plann Manage 5(4):225–239
27. Scheepmaker GM, Goverde RMP (2020) Energy-efficient train control using nonlinear bounded regenerative braking. Transp Res Part C Emerg Technol 121:102852
28. Scheepmaker GM, Goverde RMP (2021) Energy-efficient train timetabling considering capacity consumption and robustness. Euro J Transp Infrastr Res 21(4):1–42
29. Scheepmaker GM, Goverde RMP, Kroon LG (2017) Review of energy-efficient train control and timetabling. Euro J Oper Res 257(2):355–376
30. Scheepmaker GM, Pudney PJ, Albrecht AR, Goverde RMP, Howlett PG (2020) Optimal running time supplement distribution in train schedules for energy-efficient train control. J Rail Transp Plann Manage 14:100180
31. Sicre C, Cucala AP, Fernández-Cardador A, Jiménez JA, Ribera I, Serrano A (2010) A method to optimise train energy consumption combining manual energy efficient driving and scheduling. WIT Trans Built Environ 114:549–560
32. Su S, Li L, Tang T, Gao Z (2013) A subway train timetable optimization approach based on energy-efficient operation strategy. IEEE Trans Intell Transp Syst 14(2):883–893
33. Su S, Tang T, Li X, Gao Z (2014) Optimization of multitrain operations in a subway system. IEEE Trans Intell Transp Syst 15(2):673–684
34. Wang P, Goverde RMP (2016) Multiple-phase train trajectory optimization with signalling and operational constraints. Transp Res Part C Emerg Technol 69:255–275
35. Wang P, Goverde RMP (2017) Multi-train trajectory optimization for energy efficiency and delay recovery on single-track railway lines. Transp Res Part B Methodol 105:340–361

36. Wang P, Goverde RMP (2019) Multi-train trajectory optimization for energy-efficient timetabling. Euro J Oper Res 272(2):621–635
37. Wang Y, De Schutter B, Van den Boom T, Ning B (2013) Optimal trajectory planning for trains—a pseudospectral method and a mixed integer programming approach. Transp Res Part C 29:97–114
38. Wu C, Lu S, Xue F, Jiang L, Chen M, Yang J (2021) A two-step method for energy-efficient train operation, timetabling, and onboard energy storage device management. IEEE Trans Transp Electrif 7(3):1822–1833
39. Wu X, Dong H, Tse CK (2021) Multi-objective timetabling optimization for a two-way metro line under dynamic passenger demand. IEEE Trans Intell Transp Syst 22(8):4853–4863
40. Xu Y, Jia B, Li X, Li M, Ghiasi A (2020) An integrated micro-macro approach for high-speed railway energy-efficient timetabling problem. Transp Res Part C Emerg Technol 112:88–115
41. Yang X, Wu J, Sun H, Gao Z, Yin H, Qu Y (2019) Performance improvement of energy consumption, passenger time and robustness in metro systems: a multi-objective timetable optimization approach. Comput Industr Eng 137:106076
42. Ye H, Liu R (2016) A multiphase optimal control method for multi-train control and scheduling on railway lines. Transp Res Part B Methodol 93:377–393
43. Zhou L, Tong LC, Chen J, Tang J, Zhou X (2017) Joint optimization of high-speed train timetables and speed profiles: a unified modeling approach using space-time-speed grid networks. Transp Res Part B Methodol 97:157–181